Ag-Grid/Graphene Hybrid structure for Large-Scale, Transparent, Flexible Heaters

ARTICLE *in* NANOSCALE · MARCH 2015

Impact Factor: 7.39 · DOI: 10.1039/C4NR06984F

8 AUTHORS, INCLUDING:

Junmo Kang
Sungkyunkwan University

Yonghee Jang
Sungkyunkwan University

Jae-Boong Choi
Sungkyunkwan University

Doyoung Byun
Sungkyunkwan University

Supporting Information

Ag-Grid/Graphene Hybrid Structure for Large-Scale, Transparent, Flexible Heaters

Junmo Kang,[a,b,†] Yonghee Jang,[c,†] Youngsoo Kim,[d] Seung-Hyun Cho,[e] Jonghwan Suhr,[e,f] Byung Hee Hong,[a,g] Jae-Boong Choi,[a,c,*] and Doyoung Byun[c,*]

[a] *SKKU Advanced Institute of Nanotechnology (SAINT) and Center for Human Interface Nano Technology (HINT), Sungkyunkwan University, Suwon 440-746, Korea.*

[b] *Departments of Materials Science and Engineering, Northwestern University, Evanston, Illinois 60208, United States.*

[c] *School of Mechanical Engineering, Sungkyunkwan University, Suwon 440-746, Korea.*

[d] *Department of Physics and Astronomy, Seoul National University, Seoul, 151-742, Korea.*

[e] *Department of Polymer Science and Engineering, Sungkyunkwan University, Suwon 440-746, Korea.*

[f] *Department of Engergy Science, Sungkyunkwan University, Suwon 440-746, Korea.*

[g] *Department of Chemistry, Seoul National University, Seoul 143-747, Korea.*

†These authors contributed equally to this work.

* Corresponding Author, **e-mail: boong33@skku.edu and dybyun@skku.edu**

† J. Kang and Y. Jang contributed equally to this work.

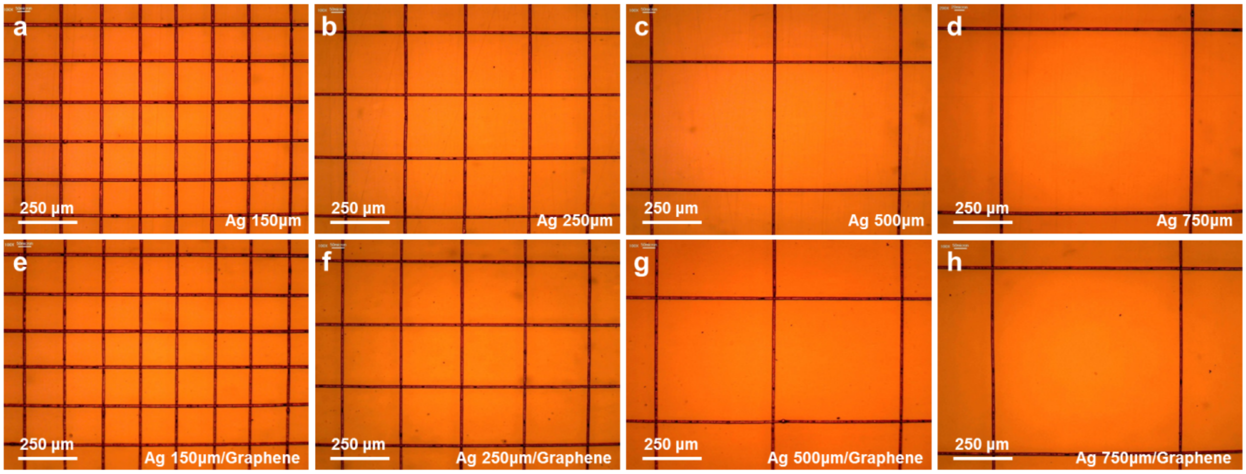

Fig. S1 The optical microscope images of the square-shaped Ag-grids at different line pitch (150, 250, 500, and 750 µm) on (a-d) PET and (e-h) graphene/PET substrates. These images are taken under the same magnification.

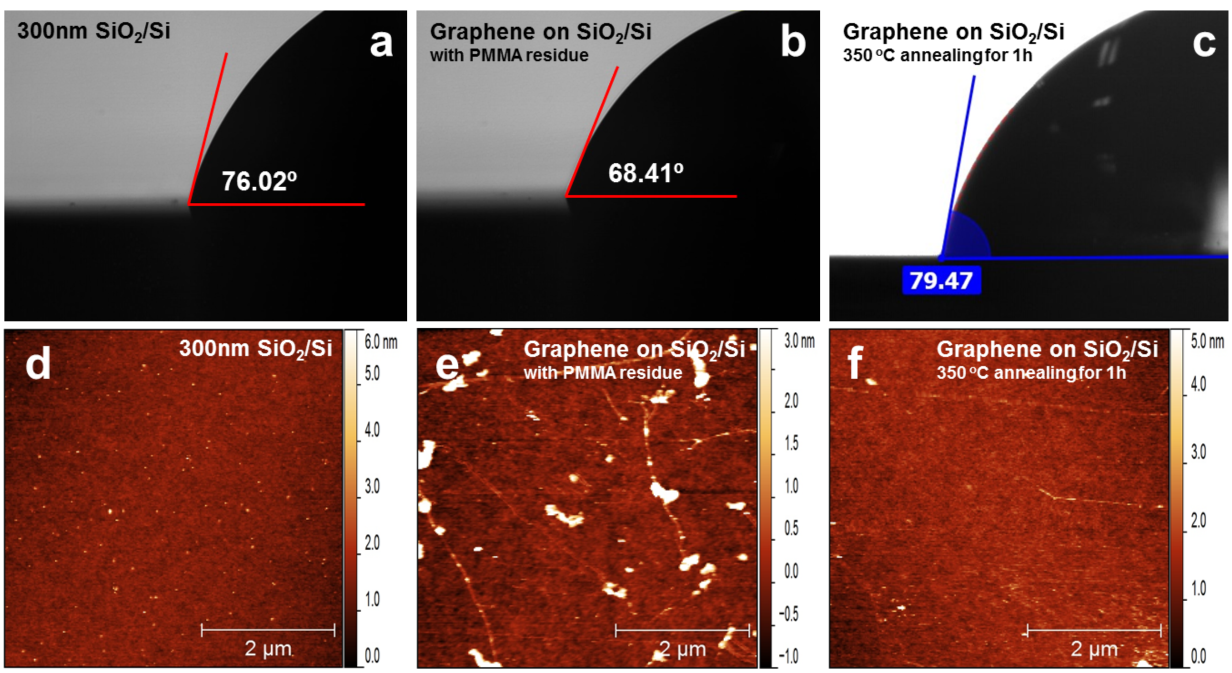

Fig. S2 (a-c) Contact angles of water droplets on (a) 300 nm SiO_2/Si wafer, (b) graphene after transferred on SiO_2/Si, and (c) graphene/SiO_2/Si after annealing in Ar/H_2 at 300 ^{o}C. (d-f) AFM images of (d) 300 nm SiO_2/Si wafer, (e) graphene after transferred on SiO_2/Si, and (f) graphene/SiO_2/Si after annealing in argon/hydrogen at 300 °C.

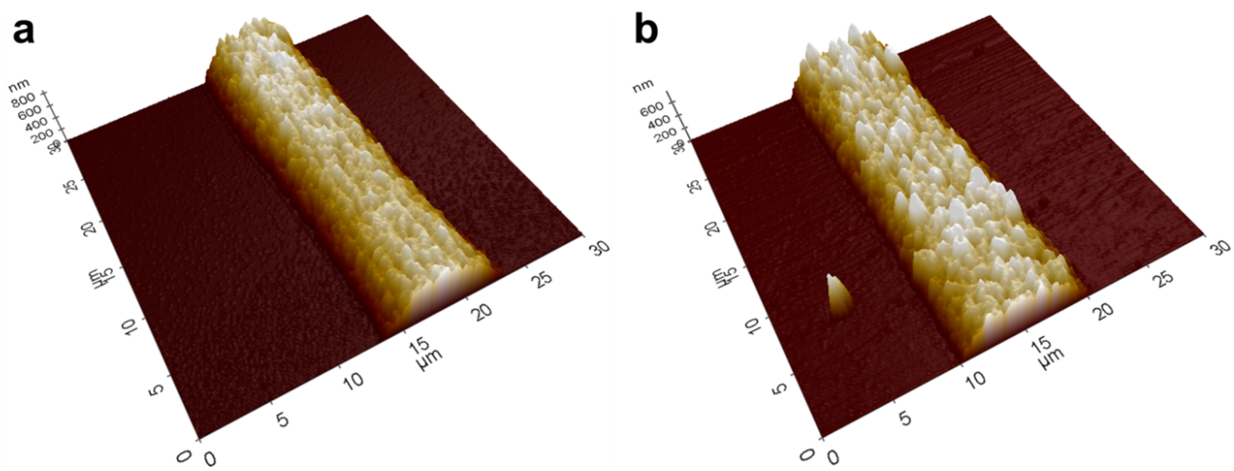

Fig. S3 3D profile by AFM images. (a) Ag line and (b) Ag line/graphene on the SiO_2/Si wafer.

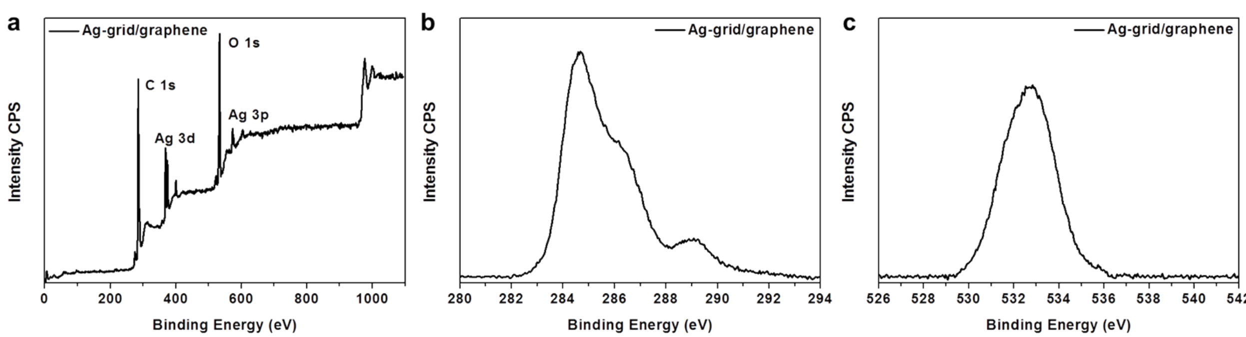

Fig. S4 XPS spectrum of Ag-grid/graphene on PET substrate. (a) Wide scan of XPS of Ag-gird/graphene on PET substrate. High resolution XPS of (b) C 1s peak and (c) O 1s peak from an Ag-grid/graphene on PET substrate.

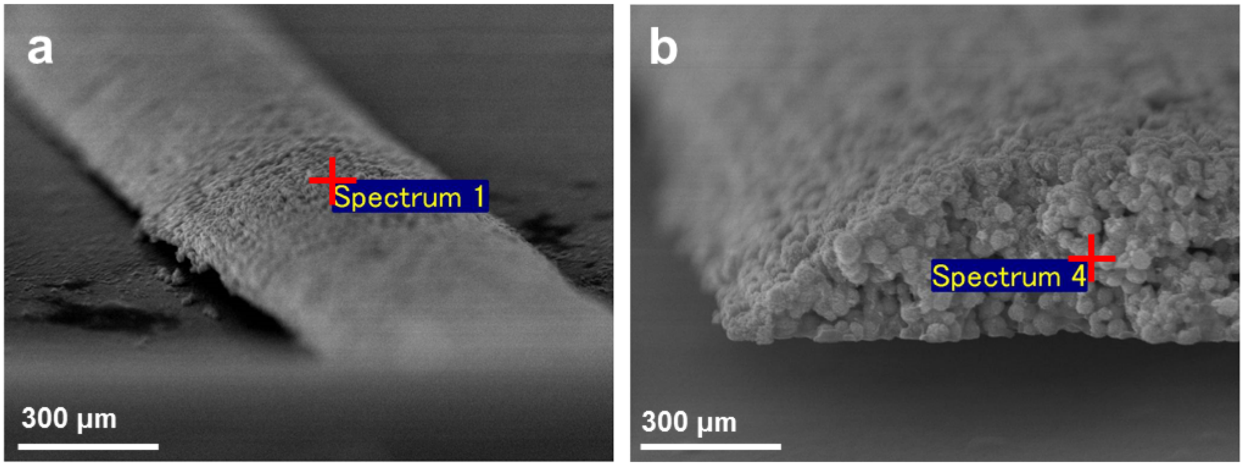

Element	Weight %	Atomic %
O K	63.00	91.99
Ag L	37.00	8.01
Totals	100.00	

Element	Weight %	Atomic %
O K	0	0
Ag L	100.00	100.00
Totals	100.00	

Fig. S5 SEM images and EDS data for (a) top and (b) middle of Ag-grid/graphene on PET substrate.

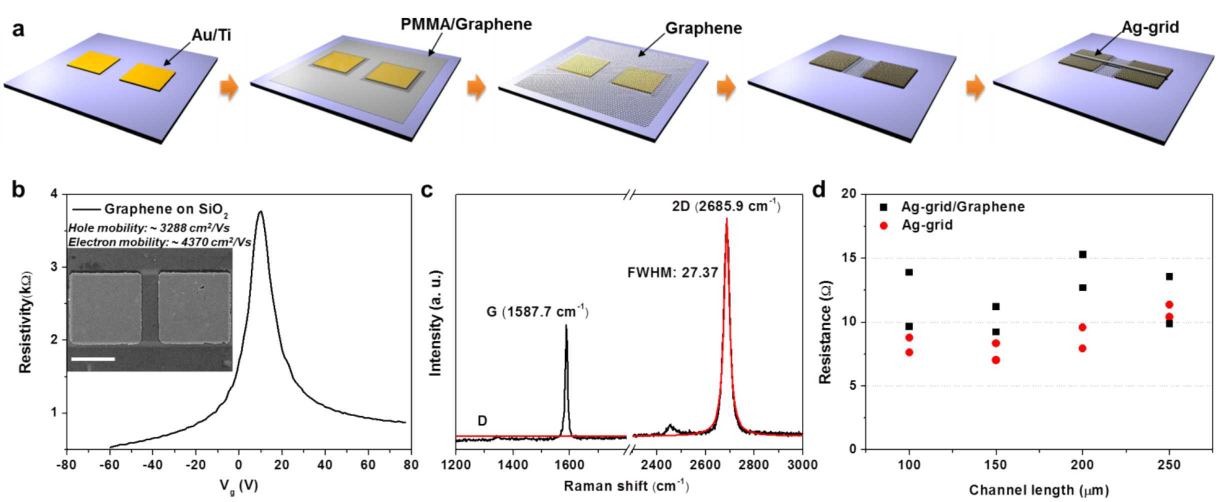

Fig. S6 Electrical and optical properties of the FET based on graphene and Ag-grid/graphene electrodes. (a) A schematic illustration of fabrication procedures of the Ag-grid/graphene electrode. (b) Resistivity-gate voltage of a graphene-based device. The left insert shows the SEM image of the graphene-based device. The scale bar in SEM image is 150 μm. The graphene-based device shows ambipolar filed effect and 10 V of dirac voltage. We determined the mobility of graphene-based device from the equation: $I_D = \frac{W\,C_i}{L} V_D \mu\,(V_G - V_T)$, where C_i = 1.08 × 10^{-8} Fcm^{-2}, V_D = 0.1 V, W = 250 μm, and L = 50 μm. (c) Representative Raman spectrum (excitation wavelength: 514nm) of the graphene film. (d) The resistance of the Ag-grid and Ag-grid/graphene as a function of the channel length.

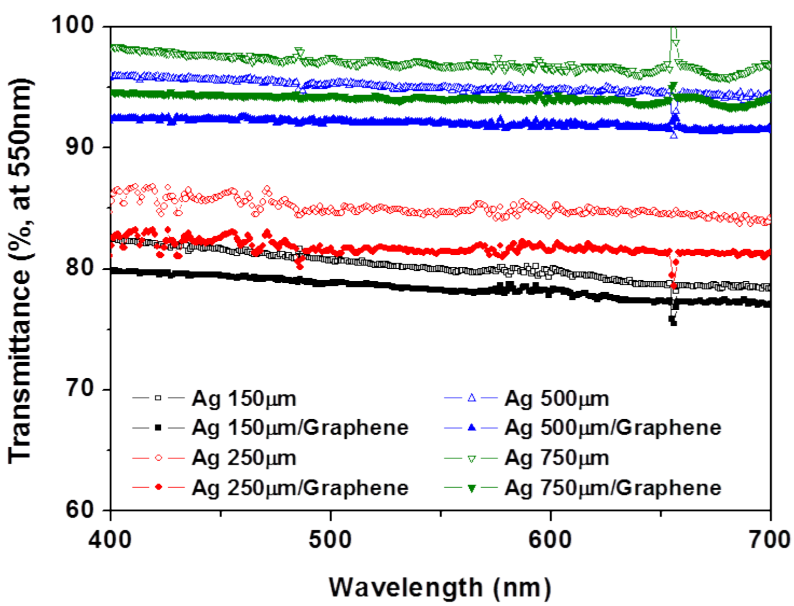

Fig. S7 Optical properties of Ag-grid and Ag-grid/graphene electrodes on PET substrates.

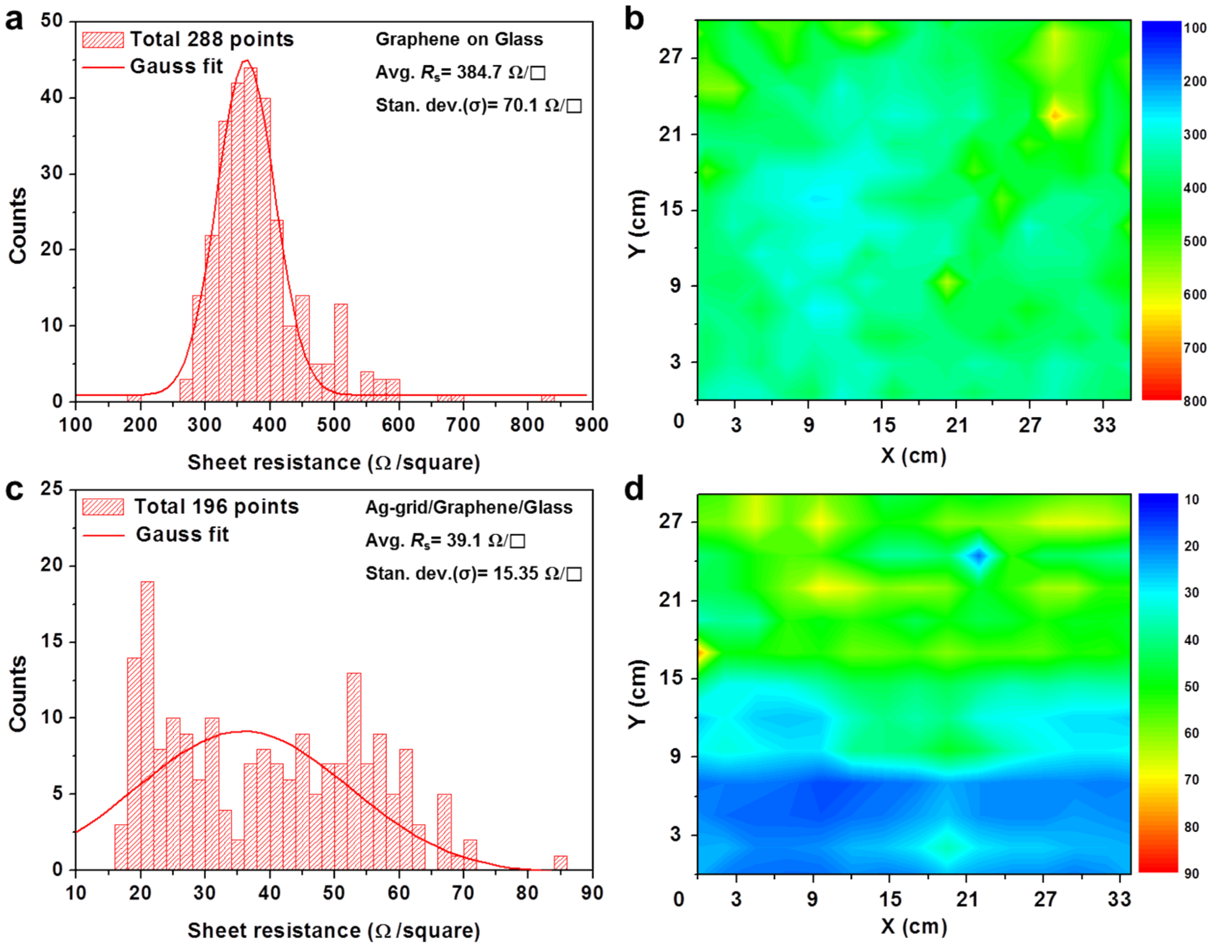

Fig. S8 Sheet resistance distribution of a large-area (a, b) graphene film and (c, d) a Ag-grid/graphene film on glass substrates. (a, c) The sheet resistance histogram of the 30 × 35 cm^2 graphene film and Ag-grid/graphene film. The sheet resistances were measured at 288 points for graphene film and at 196 points for Ag-grid/graphene film. (b, d) The corresponding spatial distribution of sheet resistances.

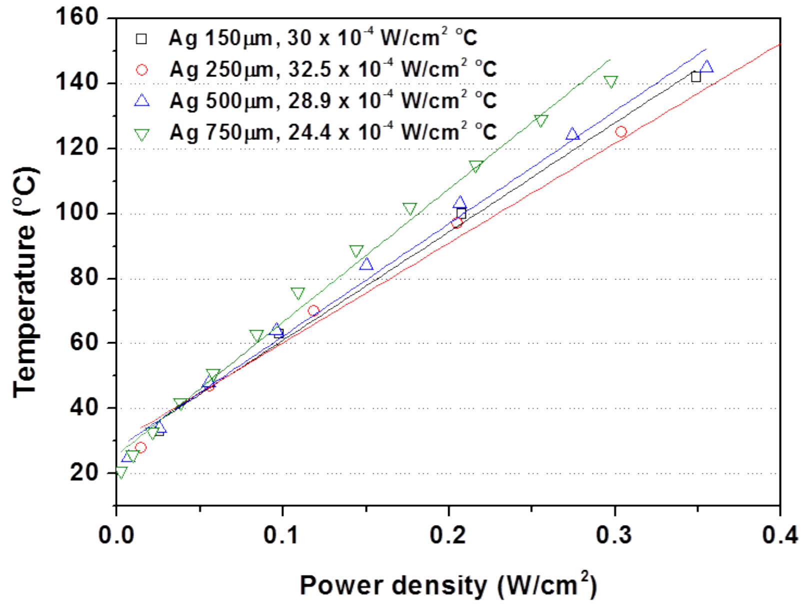

Fig. S9 Steady-state temperatures of the Ag-grid heaters as a function of input power density.

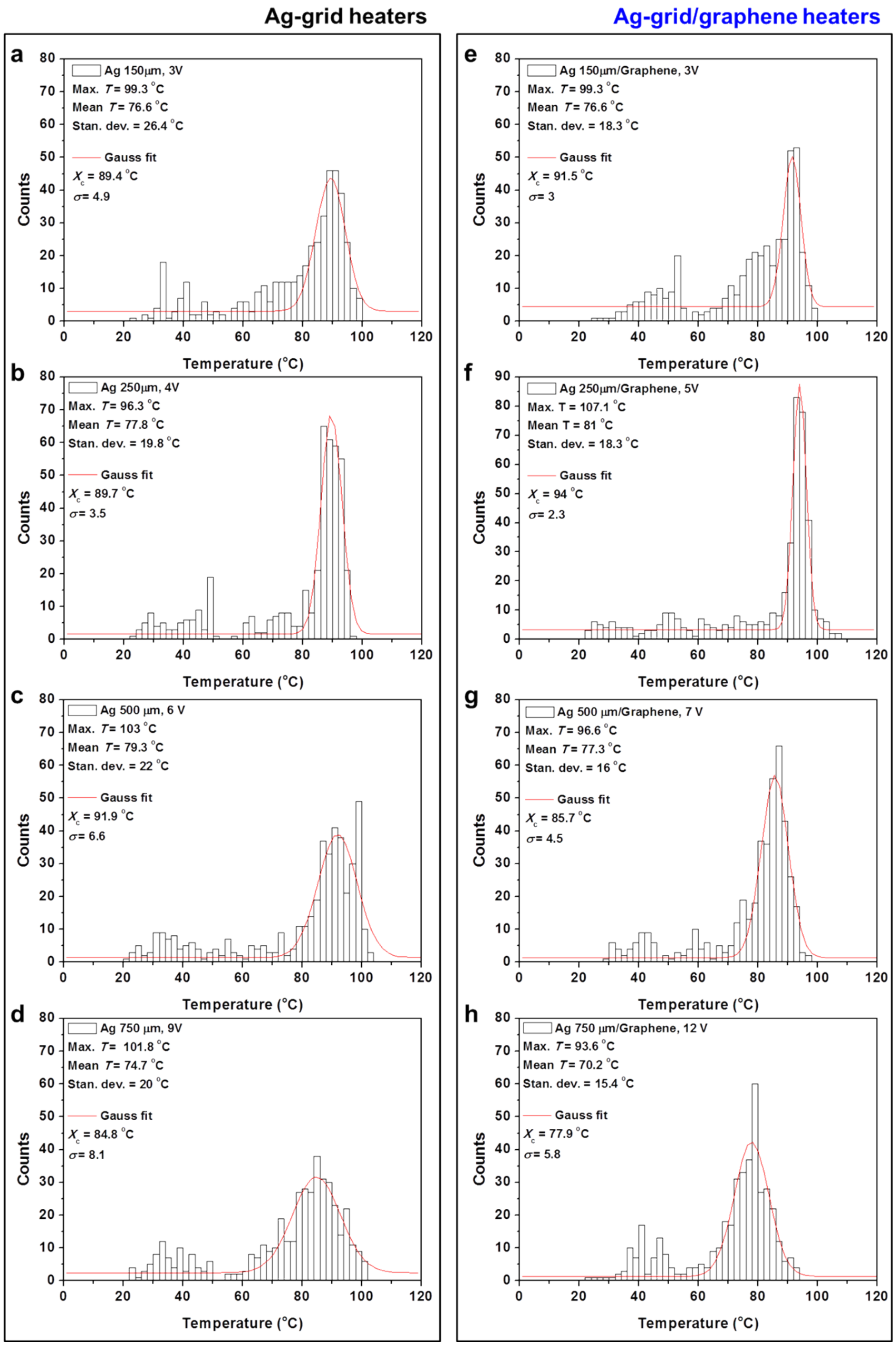

Fig. S10 Statistical analysis of the temperature distribution in the (a-d) Ag-grid and (e-h) Ag-grid/graphene heaters at approximately 100°C. All data were measured at the steady-state temperatures.

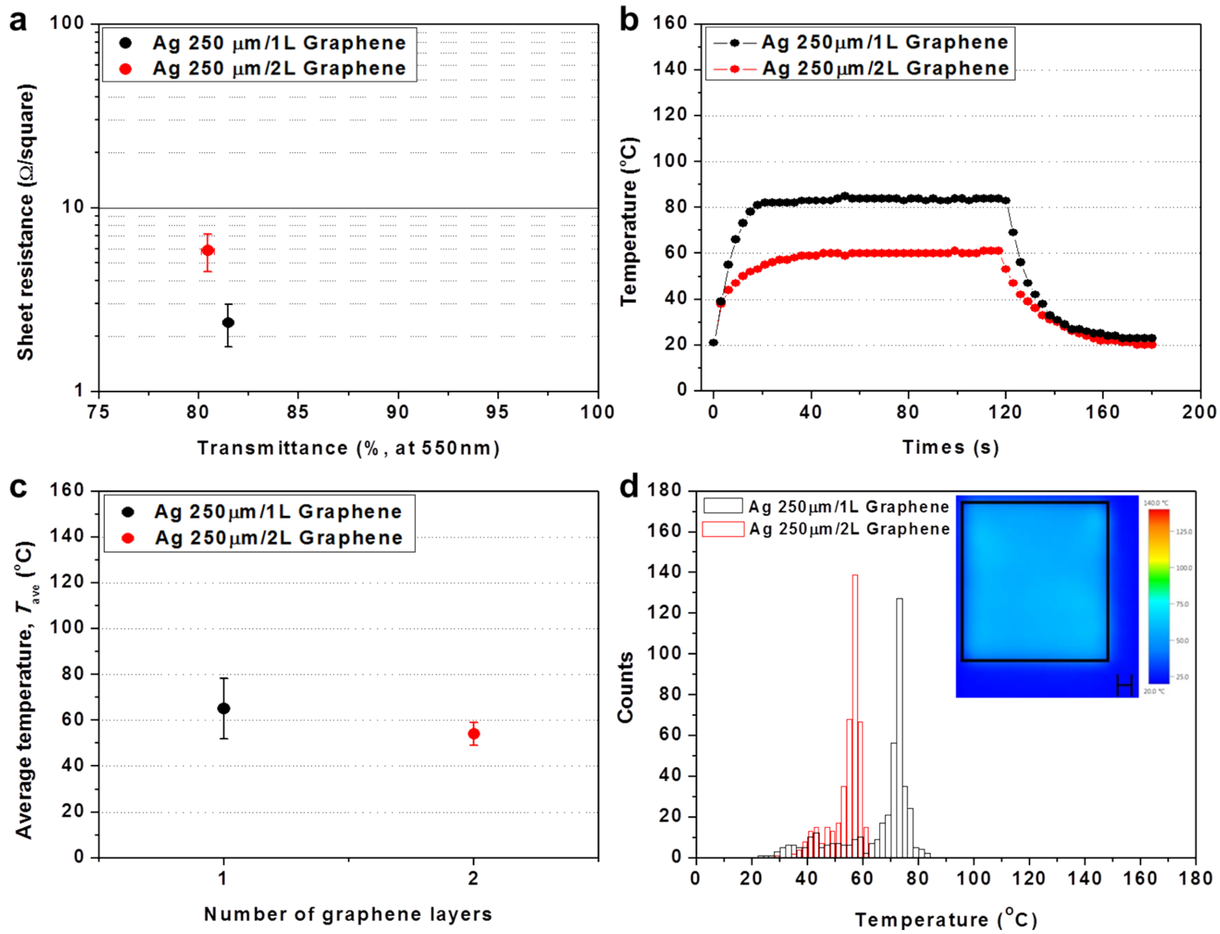

Fig. S11 Comparison of the Ag-grid/graphene hybrid films depending on the layer numbers of graphene: (a) electrical and optical properties. (b) Time-dependent temperature response. (c) The average temperature and temperature distribution. (d) Statistical analysis of the temperature distribution.